Modelling storm response on gravel beaches using XBeach-G

1 **Gerd Masselink** MSc, PhD
Professor in Coastal Geomorphology, Plymouth University, Plymouth, UK
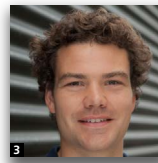
2 **Robert McCall** MSc
Researcher/Consultant, Deltares, Delft, The Netherlands

3 **Tim Poate** MSc, PhD
Post-Doctoral Research Fellow, Plymouth University, Plymouth, UK

4 **Pieter van Geer** MSc
Researcher/Advisor, Deltares, Delft, The Netherlands

Despite the clear societal importance of gravel beaches and barriers in protecting coastal areas from flooding, there are currently no reliable numerical models for predicting the morphological response of gravel beaches to storm events. This paper synthesises the results of a research project (NUPSIG) aimed at reducing this shortfall through an integrated research approach, involving field experimentation, comprehensive beach monitoring and innovative numerical modelling. In particular, the authors introduce a storm impact model for gravel beaches and barriers developed during the project (XBeach-G), present a brief validation of the model using field data and describe a user-friendly graphical user interface for the model. Finally, the model is applied in two case studies to demonstrate the use of the model in decision-making processes related to coastal flooding and beach maintenance.

Notation

A	cross-sectional area of the barrier above the still water level
b_{rel}	relative bias, defined as the model bias normalised by the measured run-up
c_f	bed friction factor
D_{50}	median grain diameter
D_{90}	90% exceedence grain diameter
d	water depth
f_s	user-defined sediment friction factor
$\bar{H}$	depth-averaged hydraulic head
H_s	significant wave height
h_{gw}	height of the groundwater surface above the bottom of the aquifer
K	hydraulic conductivity of the aquifer
k	wave number
L_m	deep water wave length
L_{model}	cross-shore model domain extent
L_{wave}	characteristic wave length
m	moment of the wave spectrum
$\bar{q}$	depth-averaged dynamic pressure normalised by the density
q_s	volumetric sediment transport rate
R_c	height of the barrier crest above the still water level
Re	Reynolds number
$R_{2\%}$	run-up level exceeded by 2% of the run-up crests
$R_{5\%}$	run-up level exceeded by 5% of the run-up crests
$R_{10\%}$	run-up level exceeded by 10% of the run-up crests
$R_{20\%}$	run-up level exceeded by 20% of the run-up crests
s	surface water–groundwater exchange flux
t	temporal coordinate
u	depth-averaged cross-shore velocity
u_*	friction velocity
u_{gw}	depth-averaged horizontal groundwater velocity
ν_h	horizontal viscosity
$w_{gw,s}$	vertical groundwater velocity at the groundwater surface
x	horizontal coordinate
β	bed angle
ϕ	phase lag angle

Maritime Engineering
Volume 167 Issue MA4

Modelling storm response
on gravel beaches using
XBeach-G
Masselink, McCall, Poate and
van Geer

θ	Shields parameter	
ρ	density of water	
ρ_s	density of the sediment	
ξ	elevation of the bed above an arbitrary horizontal plane	
ζ	free surface elevation above an arbitrary horizontal plane	

1. Introduction

Gravel barriers and beaches extend along more than 1000 km of the coastline of England and Wales and represent sustainable coastal defences that can protect low-lying back-barrier regions from flooding during storm events. They are also widespread along other high-latitude coasts (e.g. Ireland, Canada), high-relief coasts (e.g. Japan, New Zealand) and in the Mediterranean (e.g. Côte d'Azur). Their societal role is widely acknowledged, and coastal engineering structures (seawalls and groins) and management techniques (recharge, recycling and reshaping) are extensively used, at significant cost, to maintain and enhance their protective ability (e.g. Moses and Williams, 2009). Gravel is even used to create beaches, for example in Lake Montana on a small scale (Lorang, 1991), to produce sustainable coastal protection structures.

Jennings and Shulmeister (2002) define three types of gravel beaches: (a) 'pure' gravel beaches consisting of gravel-size material (D_{50} = 0·002–0·064 m) across the entire intertidal region; (b) 'composite' gravel beaches consisting of a pure gravel high-tide beach fronted by a sandy low-tide terrace; and (c) 'mixed' gravel beaches consisting of a mixture of sand and gravel sediment. Field data from all three gravel beach types are represented in this paper, but the numerical model discussed here has specifically been developed to predict the morphodynamic behaviour for the pure gravel beach type (e.g. profile response); however, the hydrodynamics predicted by the model (e.g. wave run-up) are also applicable to the mixed and composite gravel beach types.

Coastal erosion is widespread along gravel beaches in the UK (e.g. Chadwick et al., 2005; Pye and Blott, 2006, 2009) and at other locations (e.g. Komar, 2010), with erosion rates expected to increase as a result of sea-level rise and possibly enhanced storminess due to climate change. Gravel beach erosion can occur along the entire beach frontage as a result of barrier roll-over, or can be more localised where erosion along one end of the beach is accompanied by accretion at the opposite end (i.e. beach rotation). The need to understand and model morphodynamic processes on gravel beaches has been recognised by the Department for Environment, Food and Rural Affairs (Defra), which has commissioned a number of research projects concerning gravel barriers and beaches over the past few years (see projects FD1901, FD1923, FD1924 and FD1304 in Defra (2011)). The key conclusion of the most recent project Understanding Barrier Beaches (FD1924) is that regular breaching and extensive storm damage has occurred at many gravel barrier sites in the UK, and that limited scientific guidance is currently available to provide beach managers with operational management tools to predict the response of these beaches to storm conditions.

Two features in particular distinguish gravel beaches from their sandy counterparts: a steeper beach gradient and much greater sediment permeability. As a result of the steeper beach slope, waves tend to break over a shorter distance and more violently than on a sandy beach, and can result in higher wave run-up than on sandy beaches (T. Poate, G. Masselink, R. McCall et al., A new wave run-up equation for sand, gravel and mixed sand-gravel beaches, in preparation; Polidoro et al., 2013). Most of the sediment transport takes place in the swash zone, rather than the surf zone, giving rise to the development of swash morphology (berm, cusps, step; Poate et al., 2013), instead of nearshore bars, troughs and rip channels. Due to the greater permeability of gravel compared with sand, in/exfiltration effects are expected to be more significant on gravel beaches (Kirk, 1975; She et al., 2007). In particular, swash infiltration losses will be greater (Austin and Masselink, 2006), creating asymmetry in the swash transport potential, and reducing overwash volumes.

Despite a qualitative understanding of gravel barrier dynamics, engineers are not able to predict confidently the morphological response of gravel beaches to changing wave and water-level conditions. Even an ability to make predictions of the type of gravel beach response is limited. Two parametric models are currently in use for predicting storm impacts on gravel barriers (Obhrai et al., 2008). The Powell (1990) model is based on the concept of an equilibrium beach profile, while the approach of Bradbury (2002) uses a barrier inertia parameter, reflecting the balance between wave forcing and barrier resistance, to assess the occurrence of overtopping, overwashing and breaching (cf. Bradbury et al., 2005). These models are useful in their own right, but cannot be applied to predict the temporal morphological development, because actual cross-shore sediment transport rates are not considered. Numerical models developed for sandy beaches may be used to predict the morphological response of gravel beaches, but fundamental differences between sandy and gravel beach dynamics (e.g. Buscombe and Masselink, 2006; López de San Román-Blanco et al., 2006) preclude their application without significant modifications. It is therefore a necessary conclusion that there is currently no reliable numerical model available for predicting the morphological response of gravel beaches to changing wave/tide conditions over the short- to medium-term time scale (minutes to weeks).

Maritime Engineering
Volume 167 Issue MA4

Modelling storm response
on gravel beaches using
XBeach-G
Masselink, McCall, Poate and
van Geer

This paper synthesises the result of a research project specifically aimed to develop a capability to predict the response of gravel beaches to extreme wave and water-level conditions through an integrated research approach, involving field experimentation, comprehensive beach monitoring and innovative numerical modelling (NUPSIG project: New Understanding and Prediction of Storm Impacts on Gravel Beaches). Rather than developing a new model from first principles, the approach adopted here is to use an existing model that has been applied successfully to sandy beaches and modify the model for use on gravel beaches using field data. The model used as a starting point is the XBeach model (Roelvink *et al.*, 2009), which has been specifically developed to predict hurricane impacts on sandy barriers. The modified model is referred to as XBeach-G (as in XBeach-Gravel), and to enable wide use of this model by coastal managers and coastal engineers, a graphical user interface (GUI) was developed to facilitate setting up the model, and inspecting and exporting the model output.

The objectives of this paper are to describe the basic equations underpinning the XBeach-G model, present a brief validation of the model using field data, introduce the GUI and illustrate input and export options, use two case studies to demonstrate the use of the model, and outline the model capabilities and limitations.

2. XBeach-G model description

The model used in this paper, XBeach-G (McCall *et al.*, 2014; R.T. McCall, G. Masselink, T.G. Poate and J.A. Roelvink JA, Modelling storm morphodynamics on gravel beaches with XBeach-G, in preparation), constitutes a one-dimensional (cross-shore transect) extension of the XBeach storm-impact model (Roelvink *et al.*, 2009) for gravel beaches through the application of (*a*) a non-hydrostatic pressure correction term that allows wave-by-wave modelling of the surface elevation and depth-averaged flow; (*b*) a groundwater model that allows infiltration and exfiltration through the permeable gravel bed to be simulated; and (*c*) sediment transport relations that account for gravel bed load transport. The following sections address the main equations of the XBeach-G model; a full description of the hydrodynamic and morphodynamic equations is provided by McCall *et al.* (2014) and McCall *et al.* (in preparation), respectively.

2.1 Equations for surface water including short waves

XBeach-G uses a depth-averaged, non-hydrostatic extension to the standard XBeach model (Smit *et al.*, 2010) that allows XBeach-G to solve not only long (infragravity) waves but also wave-by-wave flow and surface elevation variations due to short waves in intermediate and shallow water depths (cf. SWASH model, Zijlema *et al.* (2011) and Smit *et al.* (2013)), which are of particular importance on steep, reflective gravel

beaches. Depth-averaged flow due to waves and currents is computed in XBeach-G using the non-linear shallow water equations, including a non-hydrostatic pressure term and a source term for exchange with the groundwater.

1. $$\frac{\partial \zeta}{\partial t} + \frac{\partial hu}{\partial x} + s = 0$$

2. $$\frac{\partial u}{\partial t} + u\frac{\partial u}{\partial x} - \nu_\mathrm{h}\frac{\partial^2 u}{\partial x^2} = -\frac{1}{\rho}\frac{\partial(\overline{q} + \rho g\zeta)}{\partial x} - c_\mathrm{f}\frac{u|u|}{h}$$

where x and t are the horizontal spatial and temporal coordinates, respectively, ζ is the free surface elevation above an arbitrary horizontal plane, u is the depth-averaged cross-shore velocity, $h = \zeta - \xi$ is the total water depth, ξ is the elevation of the bed above an arbitrary horizontal plane, s is the surface water–groundwater exchange flux, ν_h is the horizontal viscosity, ρ is the density of water, $\overline{q}$ is the depth-averaged dynamic pressure normalised by the density, g is the gravitational constant and c_f is the bed friction factor (computed using the Chézy equation for turbulent flow, assuming a roughness height of $3D_{90}$).

2.2 Equations for groundwater

To account correctly for upper swash infiltration losses and exfiltration effects on lower swash hydrodynamics on gravel beaches, XBeach-G computes groundwater dynamics and the exchange between groundwater and surface water using a groundwater model (McCall *et al.*, 2012). Horizontal groundwater flow in in the aquifer is computed assuming incompressible flow and the law of Darcy (1856).

3. $$\frac{\partial h_\mathrm{gw}u_\mathrm{gw}}{\partial x} + w_\mathrm{gw,s} = 0$$

4. $$u_\mathrm{gw} = -K\frac{\partial \overline{H}}{\partial x}$$

where u_gw is the depth-averaged horizontal groundwater velocity, h_gw is the height of the groundwater surface above the bottom of the aquifer, $w_\mathrm{gw,s}$ is the vertical groundwater velocity at the groundwater surface, which includes the surface water–groundwater exchange flux (s), K is the hydraulic conductivity of the aquifer and $\overline{H}$ is the depth-averaged hydraulic head. As Darcy's law is only strictly valid for laminar flow, the model approximates turbulent groundwater flow conditions using a modification of the laminar hydraulic conductivity similar to Halford (2000).

Maritime Engineering
Volume 167 Issue MA4

**Modelling storm response
on gravel beaches using
XBeach-G**
Masselink, McCall, Poate and
van Geer

5. $$K = \begin{cases} K_{\text{lam}} \sqrt{\dfrac{\text{Re}_{\text{crit}}}{\text{Re}}} & \text{Re} > \text{Re}_{\text{crit}} \\ K_{\text{lam}} & \text{Re} \le \text{Re}_{\text{crit}} \end{cases}$$

where K_{lam} is the laminar hydraulic conductivity, Re is the current Reynolds number of the interstitial flow and Re_{crit} is the critical Reynolds number for the start of turbulent flow. Thus, for turbulent interstitial flow, the hydraulic conductivity K decreases as the flow becomes more turbulent.

2.3 Equations for sediment transport and morphology

The dominant modes of sediment transport on gravel beaches are assumed to be bed load and sheet flow transport. The total gravel sediment transport is computed using a modification of the Meyer-Peter and Müller (1948) equation for bed load transport derived by Nielsen (2002).

6. $$q_s = 12(\theta - 0{\cdot}05)\sqrt{\theta}\sqrt{\left(\frac{\rho_s - \rho}{\rho}\right)gD_{50}^3}$$

where q_s is the volumetric sediment transport rate, θ is the Shields parameter, ρ_s is the density of the sediment and D_{50} is the median grain diameter. Following Fredsøe and Deigaard (1992), the Shields parameter is adjusted for bed slope effects.

7. $$\theta = \frac{u_*^2}{\left(\dfrac{\rho_s - \rho}{\rho}\right)gD_{50}}\cos(\beta)\left(1 \pm \frac{\tan(\beta)}{\tan(\phi)}\right)$$

where u_* is the friction velocity, β is the bed angle and ϕ is the angle of repose of the sediment.

To account for boundary layer expansion and contraction in the swash, pressure gradient effects and the presence of turbulent fronts, the friction velocity is computed using the approximation of Nielsen (2002).

8. $$u_* = \sqrt{\frac{f_s}{2}\left(\cos(\phi)u + \frac{T_{\text{m}-1,0}}{2\pi}\sin(\phi)\frac{\partial u}{\partial t}\right)}$$

where f_s is a user-defined sediment friction factor of the order of 0·01, $T_{\text{m}-1,0}$ is the offshore spectral period based on the first negative moment of the energy spectrum and ϕ is a user-defined phase lag angle of the order of 30°.

Bed level changes are computed due to gradients in sediment transport.

9. $$\frac{\partial \xi}{\partial t} + \frac{1}{1-n}\frac{\partial q_s}{\partial x} = 0$$

where ξ is the elevation of the bed above an arbitrary horizontal plane.

Finally, slope collapse and slumping is approximated by avalanching sediment downslope when the bed slope exceeds the angle of repose.

10. $$\left|\frac{\partial \xi}{\partial x}\right| > \phi \ \text{slumping}$$
$$\left|\frac{\partial \xi}{\partial x}\right| \le \phi \ \text{no slumping}$$

3. Validation of XBeach-G

Extensive validation of XBeach-G was conducted using field and laboratory data. Specific aspects of the validation include the transformation of waves through the narrow surf zone and lower swash zone, wave run-up statistics, interactions between the swash flow and the beach groundwater table, and the beach morphological response in the swash, overtopping and over-wash regimes. Extensive validation of the model has been presented by McCall et al. (2012, 2013, 2014, in preparation) and Poate et al. (in preparation); here, some of the key validation outputs are presented, focusing on the ability of the model to predict vertical run-up, the occurrence of overwash and morphological response.

3.1 Wave run-up

Storm response on gravel barriers primarily depends on the vertical wave run-up in relation to the elevation of the barrier crest; therefore, a numerical model for predicting storm impacts on a gravel beach must be able to predict run-up characteristics confidently. Data on wave run-up levels were collected from a wide range of sources, including a cross-shore array of bed-level sensors deployed during a large-scale gravel barrier experiment in the delta flume (BARDEX experiment; Masselink and Turner, 2012; Williams et al., 2012) and on a gravel beach in south Cornwall (Loe Bar; Poate et al., 2013), and pixel time stacks derived from video data during the field experiments carried out over the years on a number of gravel sites in the UK (Chesil, Hayling, Seascale, Slapton Sands, Westward Ho!; see McCall et al. (2014) for a detailed description of these field experiments).

To compare predicted and measured run-up levels, XBeach models were set up for a measurement series of the BARDEX experiment, as well as wave events at six gravel beaches along the UK coast (cf. Poate et al., in preparation). Each simulation was run for the duration of maximum tide levels and contiguous camera or bed-level sensor data, which was generally in the order of 0·5–1 h. Run-up exceedence levels ($R_{2\%}$, $R_{5\%}$, $R_{10\%}$ and $R_{20\%}$) were computed from 15–20 min sections of observed and modelled shoreline time series. To investigate the sensitivity of the modelled run-up levels to the selection of random wave components at the model boundary, each XBeach simulation was run ten times using a

Maritime Engineering
Volume 167 Issue MA4

Modelling storm response
on gravel beaches using
XBeach-G
Masselink, McCall, Poate and
van Geer

new random wave time series of the imposed offshore wave
spectrum.

Measured and modelled run-up levels at all sites are shown in
Figure 1. Vertical error bars in the figure represent variations
in the modelled run-up levels due to variations in the random
wave time series applied at the model boundary. Horizontal
error bars represent the variation in measured run-up data
across multiple cross-shore profiles. The figure shows very
good correspondence and little scatter (low scatter index; SCI)
between measured and modelled run-up levels for all excee-
dence probabilities and at all gravel beaches. Importantly, the
model shows practically no systematic relative bias (defined as
the absolute bias, normalised by the measured run-up; b_{rel}) in
the computation of the extreme run-up levels. There is a

suggestion that there is more bias in the Chesil Beach data,
but these data are at the high-energy end of field observations
with vertical run-up up to 12 m where any bias is more
apparent when the data are plotted on a linear scale.
Variations in modelled and measured run-up levels due to
variations in the imposed wave time series and cross-shore
camera pixel stacks are of the order of 1 m (20%) for run-up
levels over 5 m.

3.2 Comparison with BIM and documented storm impacts

The barrier inertia model (BIM; Bradbury, 2002) relates
the probability of overwash on gravel beaches to the wave
steepness of the incident waves S_w, and the dimensionless
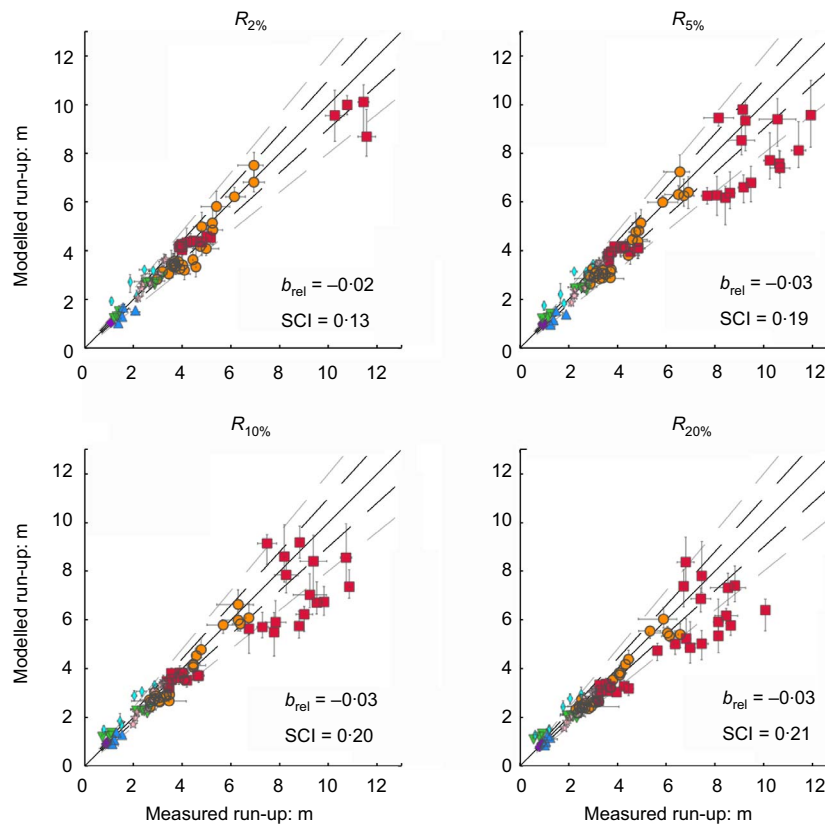barrier inertia parameter BI, defined as

Figure 1. Comparison of measured (horizontal axis) and modelled
(vertical axis) run-up heights (vertical run-up relative to still water
level) at Chesil Beach (red squares; from pixel stacks), Loe Bar
(orange circles; from bed-level sensors), Seascale (blue upward
triangles; from pixel stacks), Slapton Sands (green downward
triangles; from pixel stacks), Westward Ho! (cyan thin diamonds;
from pixel stacks), Hayling Island (pink pentagons; from pixel stacks)
and the BARDEX experiment (violet diamonds; from bed-level
sensors). The solid black line indicates a perfect 1:1 relationship, and
the dashed black and grey lines indicate a 10% and 20% deviation
from the perfect relationship, respectively. $R_{2\%}$, $R_{5\%}$, $R_{10\%}$ and $R_{20\%}$
refers to 2%, 5%, 10% and 20% exceedance run-up height,
respectively: SCI, scatter index; b_{rel}, relative bias. Figure adapted
from McCall et al. (2014) and Poate et al. (in preparation)

Maritime Engineering
Volume 167 Issue MA4

**Modelling storm response
on gravel beaches using
XBeach-G**
Masselink, McCall, Poate and
van Geer

11. $\quad S_w = \dfrac{H_s}{L_m}$

12. $\quad \text{BI} = \dfrac{R_c A}{H_s^3}$

where H_s is the significant wave height measured at 6–8 m water depth, L_m is the deep-water wave length computed using the mean wave period, R_c is the freeboard, or height of the barrier crest above still water level, and A is the cross-sectional area of the barrier above the still-water level. From analysis of laboratory and field data, Bradbury (2000) found barrier overwash is unlikely to occur when

13. $\quad \text{BI} > 0{\cdot}0006 S_w^{-2{\cdot}54}$

Although the BIM is used in many locations in the UK, the data used to derive the threshold overwash relation are specific to the site and conditions where they were measured (Hurst Spit in the south of England). The model may therefore not be valid for other sections of the coast of the UK.

A series of 22 documented storm impacts on gravel barriers and three BARDEX physical model experiments (Williams *et al.*, 2012) have been hindcast in order to validate the XBeach model approach (see McCall *et al.* (2014) for a detailed description of these cases). In these hindcast simulations, the barrier geometry is parameterised using documented topographic and bathymetric data to estimate the toe depth, beach slope, seabed slope, crest height and barrier width, and a combination of observations and estimates is used to parameterise the hydraulic conductivity of the gravel barriers. The hindcast models are forced using documented maximum wave conditions and surge levels when available, and estimates combined with sensitivity bands when accurate data are not available. The model was run without updating the barrier morphology only to model the hydrodynamics, and the key model output that indicates the occurrence and extent of overwash is the water discharge across the barrier crest Q_{crest}. Extensive XBeach simulations using idealised barrier morphology and a range of forcing conditions, supported by engineering guidelines (Simm, 1991), suggest that $Q_{crest} = 20$ l/m/s can be used to separate non-overwash and overwash conditions (McCall *et al.*, 2013).

The documented barrier storm response of the 25 hindcast events is categorised, based on the observed profile change and the amount of back-barrier flooding, into four levels of response: (*a*) rollback and severe overwash; (*b*) overwash damage and crest lowering; (*c*) overtopping and crest build-up; and (*d*) scour with no change to crest. The simulated overtopping discharges in the hindcast simulations are plotted in

Figure 2 according to the location of the storm event in BIM parameter space and according to the classification of the barrier storm response (see the figure caption for hindcast event codes).

- Breach and severe overwash (Figure 2(b)): HS, BE10 and C79 are classified as barrier breaching or severe overwash events (Figure 2(b)). HS and BE10 showed significant lowering and retreat of the crest and flooding of the hinterland. C79 also showed severe flooding of the hinterland and lowering of the crest, but no barrier retreat. XBeach predicts overtopping discharge rates greater than 100 l/m/s at HS and BE10, and over 20–100 l/m/s at C79. All three events would be classed as overwash events in the XBeach model according to the threshold values found in the model calibration. Although HS and BE10 are both below the BIM overwash threshold, C79 is located above the threshold curve and would therefore not be predicted to be an overwash event by the BIM.
- Overwash damage to the back barrier (Figure 2(c)): Overwash events are identified by damage on the back barrier and limited flooding of the hinterland. These events include C78, which caused some flooding behind the barrier, S01, which caused significant damage to the main road located on the barrier, and five separate storms between 1994 and 2000 at Medmerry (MMo). The XBeach model correctly predicts the possibility of overwash ($Q_{crest} > 20$ l/m/s) at SL01, and overwash for two storm events at Medmerry. However, C78 and the three other Medmerry storms are predicted to have an overtopping discharge less than 20 l/m/s and would therefore incorrectly be classed as non-overwash events. None of the storms in this category would, however, be predicted as possible overwash events by the BIM.
- Overtopping and crest build-up (Figure 2(d)): Overtopping events are classified as events during which the crest builds up (increase in crest elevation), the extent of the morphological change just reaches the crest, or the documentation describes occasional waves overtopping the crest. These include S04, HI and BE1. The XBeach model predicts overtopping discharges less than 20 l/m/s at all these sites and are therefore correctly classified as non-overwash events. The model does predict limited overtopping of the barrier crest (2–20 l/m/s) at SL04 and HI, which corresponds with the notion of occasional waves overtopping the crest.
- Beach erosion with no change to the crest (Figure 2(e)): The final classification is for storm events that affected the beach, but did not reach the crest. These events are called erosion events, and include three storms at Medmerry (MMs), four storms at Loe Bar (LB), the four largest storms each year between 2007 and 2010 at Chesil Beach (C07) and BC1. In a similar fashion to the overtopping events, the overwash discharge hindcast by the XBeach
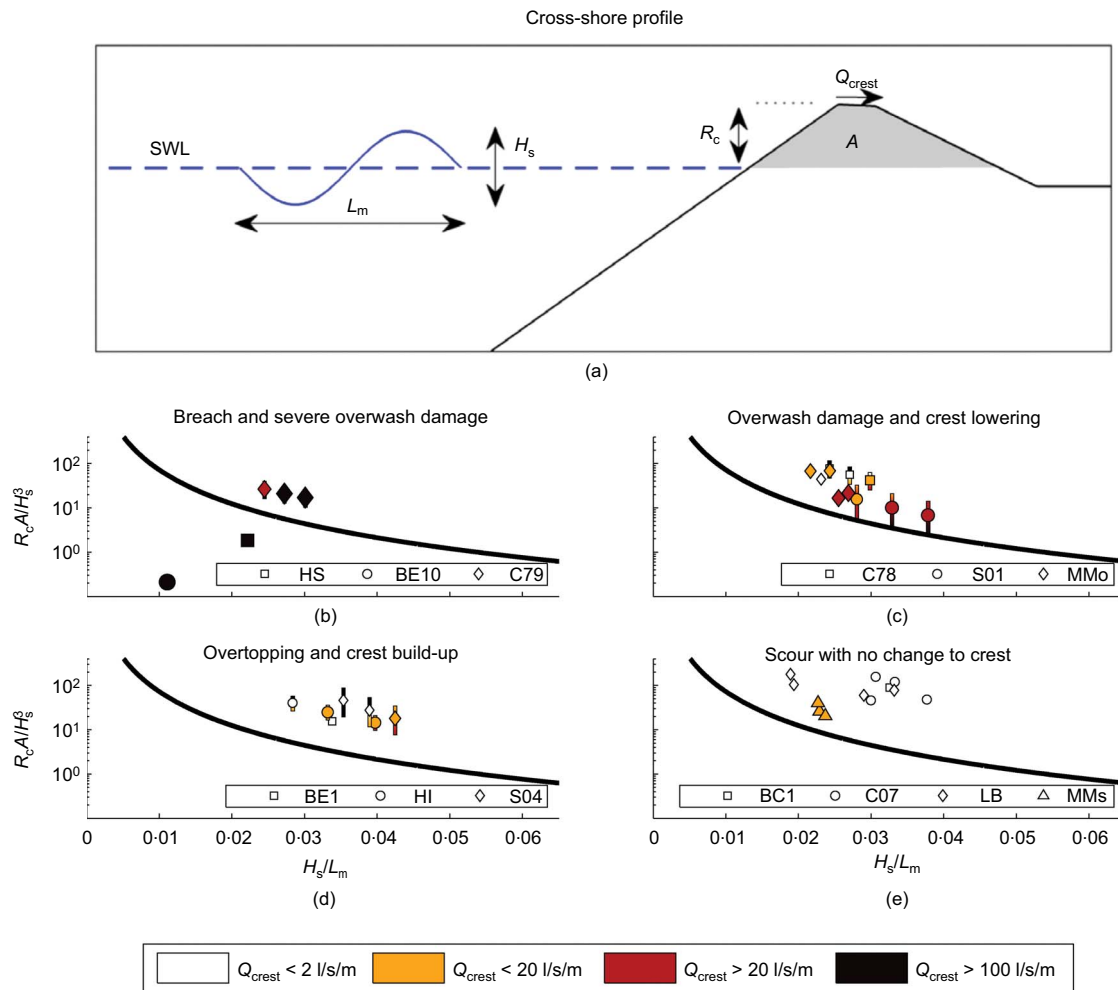
Maritime Engineering
Volume 167 Issue MA4

Modelling storm response
on gravel beaches using
XBeach-G
Masselink, McCall, Poate and
van Geer

Figure 2. Simulated overtopping discharges across the barrier crest (Q_{crest}) for hindcast tests. (a) Definition sketch of the barrier inertia model (BIM); (b–e) comparison of the performance of the BIM (Equation 14) and XBeach-G with observations. The black curve in (b–e) represents the BIM (Equation 13); according to the BIM, overwash is unlikely to occur in the parameter space above the black curve. Marker colours relate to the simulated overtopping volumes across the barrier crest Q_{crest} in XBeach-G. Twenty-five cases have been hindcasted: HS, Hurst Spit 1989; BE10, BARDEX E10; C79, Chesil Beach 1979; C78, Chesil Beach 1978; S01, Slapton Sands 2001; MMo, Medmerry 1994–2000; HI, Hayling Island 2005; S04, Slapton Sands 2004; BC1, BARDEX C1; C07, Chesil Beach 2007–2010; LB, Loe Bar 2011–2012; MMs, Medmerry 1993–2002. Note that C79, C78, S04, HI and S01 have multiple markers to show the range of uncertainty in the boundary conditions. Where sensitivity simulations have been carried out with equal wave steepness, error bars indicate the range of simulated Q_{crest} and BI values. Note that the vertical scale in Figure 2 is logarithmic: SWL, still water level. Figure adapted from McCall et al. (2013)

model is less than 20 l/m/s, and would therefore correctly be classified as non-overwash events. All events except the storms at Medmerry are predicted to have less than 2 l/m/s overtopping discharge, which corresponds with the notion of no waves reaching the crest.

The validation hindcast simulations show that the XBeach model correctly predicts the possibility of overwash in six out of ten overwash storm events. Although the absolute accuracy

of the XBeach model overwash prediction is only 60% in this validation dataset, the XBeach model still appears to improve on the BIM, which only identifies two overwash events. The majority of incorrect predictions in the XBeach model are for storm events at Medmerry (three incorrect predictions of erosion or overtopping instead of overwash and three incorrect predictions of overtopping instead of erosion), suggesting that the natural system at Medmerry is not well described by the XBeach model, or by the documented storm data.

Maritime Engineering
Volume 167 Issue MA4

**Modelling storm response
on gravel beaches using
XBeach-G**
Masselink, McCall, Poate and
van Geer

3.3 Comparison with field observations of barrier overwash

The ability of the XBeach-G model to simulate gravel barrier overwash and rollback is examined through the hindcast of the morphodynamic response of the Sillon de Talbert barrier on the north coast of Brittany (Figure 3(a)) to a large sluicing overwash event caused by storm Johanna (10 March 2008). During this storm event, which occurred in conjunction with the

(a)
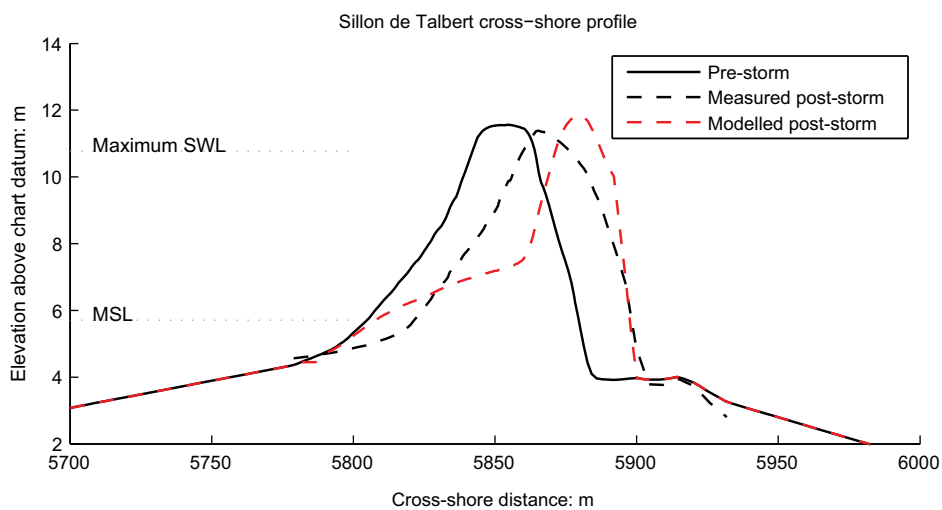
(b)

Figure 3. (a) Aerial photograph of the 3 km-long gravel barrier of Sillon de Talbert on the north coast of Brittany, France (source: Bingmap). (b) Cross-shore profile of Sillon de Talbert 6 months before storm Johanna (solid black line), cross-shore profile measured 6 months after the storm (dashed black line) and computed post-storm cross-shore profile (solid orange line). The black dotted lines indicate mean sea level (MSL) and the maximum still water level (SWL) reached during storm Johanna

Maritime Engineering
Volume 167 Issue MA4

Modelling storm response
on gravel beaches using
XBeach-G
Masselink, McCall, Poate and
van Geer

spring tide, offshore wave heights reached 9·5 m with peak wave periods of 16 s, leading to barrier rollback of approximately 15 m along the central section of the barrier (see Stéphan *et al.* (2012) and Stéphan *et al.* (2010) for a detailed description of this storm event and its impact on the barrier).

The impact of storm Johanna on the barrier is modelled in XBeach-G using topographic, bathymetric and hydrodynamic forcing conditions provided by l'Université de Bretagne Occidentale (Stéphan and Suanez, personal correspondence). Topographic data of the barrier consist of supratidal and intertidal differential GPS measurements of the barrier measured in September 2007 (prior to storm Johanna) and September 2008 (after storm Johanna; Stéphan, personal correspondence). These data are supplemented with LiDAR data of the intertidal beach measured in 2002 (Boersma and Hoenderkamp, 2003) and bathymetry data provided by the Service Hydrographique et Océanographique de la Marine. Time series of the storm surge level were derived from surge measured at the Roscoff tide gauge, located approximately 65 km from the study site, alongside tidal predictions at the location of the barrier. Wave conditions offshore of the barrier were extracted from a nested WAVEWATCH III model, forced by European Centre for Medium-Range Weather Forecasts wind fields. Model validation results on buoys off Brittany indicate an overall RMSE of 12% for wave height with a bias less than 2% (Ardhuin and Accensi, 2011).

For the purpose of this study, one cross-shore transect in the central section of the Sillon de Talbert barrier is modelled in XBeach-G. The simulation is started at the first low tide of 10 March 2008 and runs until the first low tide of 13 March 2008.

Wave, tide and surge boundary conditions derived from the data provided by l'Université de Bretagne Occidentale are imposed at an offshore depth of 20 m below mean sea level (MSL), see Figure 4. As no quantitative data are available on the grain size and hydraulic conductivity of the barrier, the median grain size is estimated to be 8 cm (cf. Chanson, 2006), and the hydraulic conductivity (K_{lam}) and critical Reynolds number for turbulence are set to 0·40 m/s and 80, respectively, analogous to the value found experimentally by Heijne and West (1991) for Portland, Chesil Beach. Following calibrated values found for Chesil Beach, the sediment friction factor (f_s) is set to 0·01 and the phase lag angle (ϕ) is set to 25°.

The cross-shore profile change due to storm Johanna, simulated by XBeach-G, is shown in Figure 3(b) alongside the cross-shore profile measured 6 months after the storm (September 2008). Due to the long duration between simulated storm and the post-storm measurements, the modelled cross-shore profile change cannot be directly compared with the measured change. However, the observed barrier rollback can be attributed to storm Johanna, which was the largest storm event in this period (Stéphan *et al.*, 2010). In a qualitative sense, the result shows that the model is able to reproduce the observed barrier rollback behaviour well, with a clear retreat of the supratidal and upper intertidal barrier.

In a quantitative sense, the model predicts bulk morphological change parameters well. The computed washover volume in the XBeach-G model is 138 m³/m, compared with 129 m³/m found in the measurements, in which washover volume is defined as the volume of material exceeding the initial bed level landward
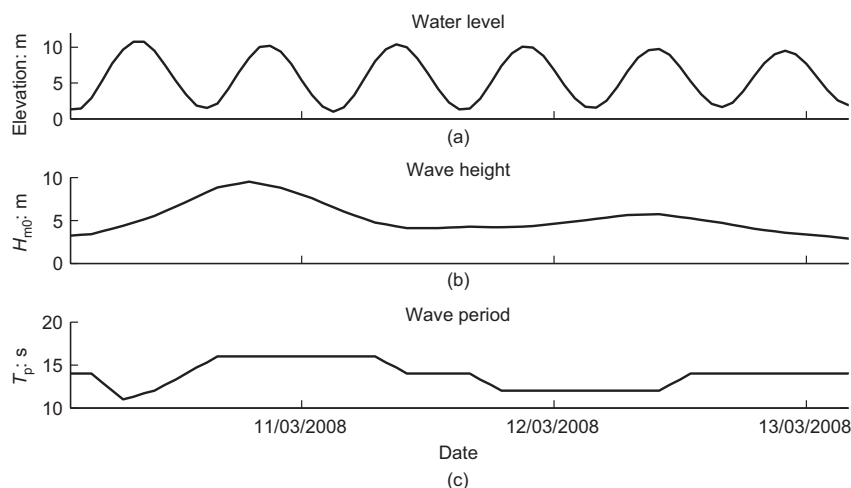

Figure 4. Time series of tide and surge levels (a), significant wave height (b) and peak wave period (c) applied in the XBeach-G simulation of storm Johanna

Maritime Engineering
Volume 167 Issue MA4

Modelling storm response
on gravel beaches using
XBeach-G
Masselink, McCall, Poate and
van Geer

of the crest. The landward movement of the centre of mass of the gravel barrier above its base at an elevation of 4 m in the XBeach-G model is 14·1 m, close to the 15·7 m found in the measurements. The accuracy of the bulk parameters is represented by a high Brier skill score (0·74) for the computed bed level change compared with the measured bed level change.

Despite good representation of the bulk morphological change parameters characterising the gravel barrier response, it is clear that the model does not represent the details of the post-storm profile equally well. The landward migration of the barrier crest is overestimated by approximately 10 m (57% of the measured migration) and the model predicts a slight increase in the crest height (0·5 m), instead of a slight lowering (0·2 m) found in the measurements. Finally, the development of the lower intertidal section of the gravel barrier is not well represented, which may be partly due to the long period between the storm and the post-storm profile measurements that is not simulated in the XBeach-G model, during which waves may have restructured this part of the profile. It should be noted that due to uncertainties in the forcing conditions (wave height and period) and barrier composition (grain size and hydraulic conductivity), as well as the long duration between the pre-storm and post-storm survey, the model was not calibrated further to reproduce better the observed barrier profile.

4. Graphical user interface

To encourage the use of XBeach-G for practical application by coastal managers, a GUI was developed that enables users to set up, run and analyse XBeach-G models. This GUI is built as a plug-in of the Delta Shell framework described by Donchyts and Jagers (2010).

4.1 Input

Figure 5 gives an overview of the model views the XBeach-G GUI offers for specifying various kinds of input. The views enable specification of the initial situation, as well as hydro-dynamic forcing at the offshore boundary and calculation parameters. This functionality is covered by the following views.

- Profile: allows the user to specify the initial cross-shore (bed) profile of the calculation. In 'characteristics' mode, the user can enter morphometric characteristics of a gravel barrier (e.g. barrier height, width of the crest, beach gradient) on the basis of which the GUI designs an initial barrier profile. In 'coordinates' mode, the user is allowed to specify the profile by means of manually entering cross-shore and elevation coordinates. A profile file with coordinates can also be directly imported. The GUI automatically generates a computational grid that best fits the initial profile and can be steered in this view.
- Tide: provides tools to specify a time series of the water level at the offshore boundary of the model. A tidal signal

can be created by means of a tide generation dialogue box in which phase and amplitude can be specified, and a constant storm surge level can be added to the tidal signal. Alternatively, the water level time series can be entered manually or imported.
- Waves: consists of a table that shows a time series of spectral specification of incident waves that will be used at the offshore boundary. A single wave spectrum or a time series of wave spectra can be entered. The spectral parameters to be specified include significant wave height H_s, peak wave period T_p, JONSWAP peak enhancement factor γ and directional spreading S. A bimodal wave spectrum can be specified by defining two sets of values for H_s, T_p, γ and S.
- Parameters: offers the ability to specify values for time management (run duration and time step), initial conditions (groundwater level and elevation of bottom of aquifer), sediment characteristics (sediment size and hydraulic conductivity), option to update morphology or not, and sediment transport parameters.

4.2 Output

Once the specified model has been run, the XBeach-G GUI offers tools to analyse the model results. Figure 6 shows two of the available output screens, consisting of the following.

- Cross-shore: provides a cross-shore slice of the calculated output at a specific point in time. Time navigation controls add the possibility to navigate through time and visualise the development of the output variables over the cross-section in time. A very large selection of output variables is available for plotting (e.g. water surface, ground water level, cross-shore velocity, water discharge across the barrier).
- Time series: shows the development of the output variables in time at a specific location along the profile. When opening both cross-shore and time series views simultaneously, the user can navigate the cross-shore position of the time series output in the cross-shore output view. As in the cross-shore view, a very large number of output variables can be selected for plotting.

4.3 Accessing the XBeach-G code and running the model outside the GUI

Apart from running XBeach-G calculations inside the GUI environment, it is also possible to run calculations without the help of the GUI. To that end the user can specify model input in a text file and provide that to the calculation engine. Running a calculation without the GUI offers more flexibility to change settings or input specification as some model settings are not accessed through the GUI. The GUI offers an export option that allows the user to export a model set-up that was generated through the GUI. The model input, including the
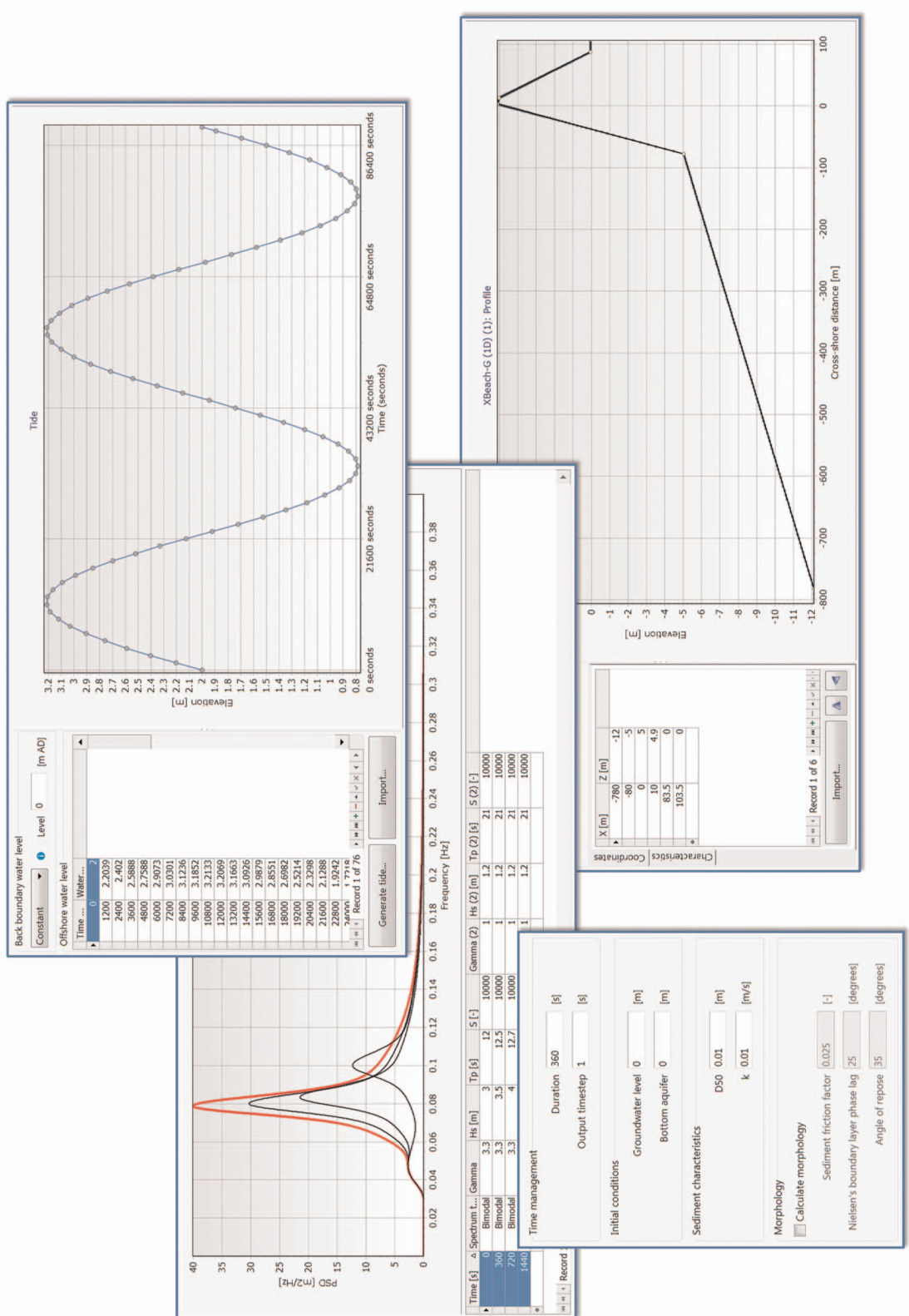
Figure 5. An overview of the GUI views that allow specifying input for an XBeach-G model. It includes profile specification (lower-right corner), tide specification (upper-right corner), wave spectra time series (middle left) and additional parameters (lower-left corner)
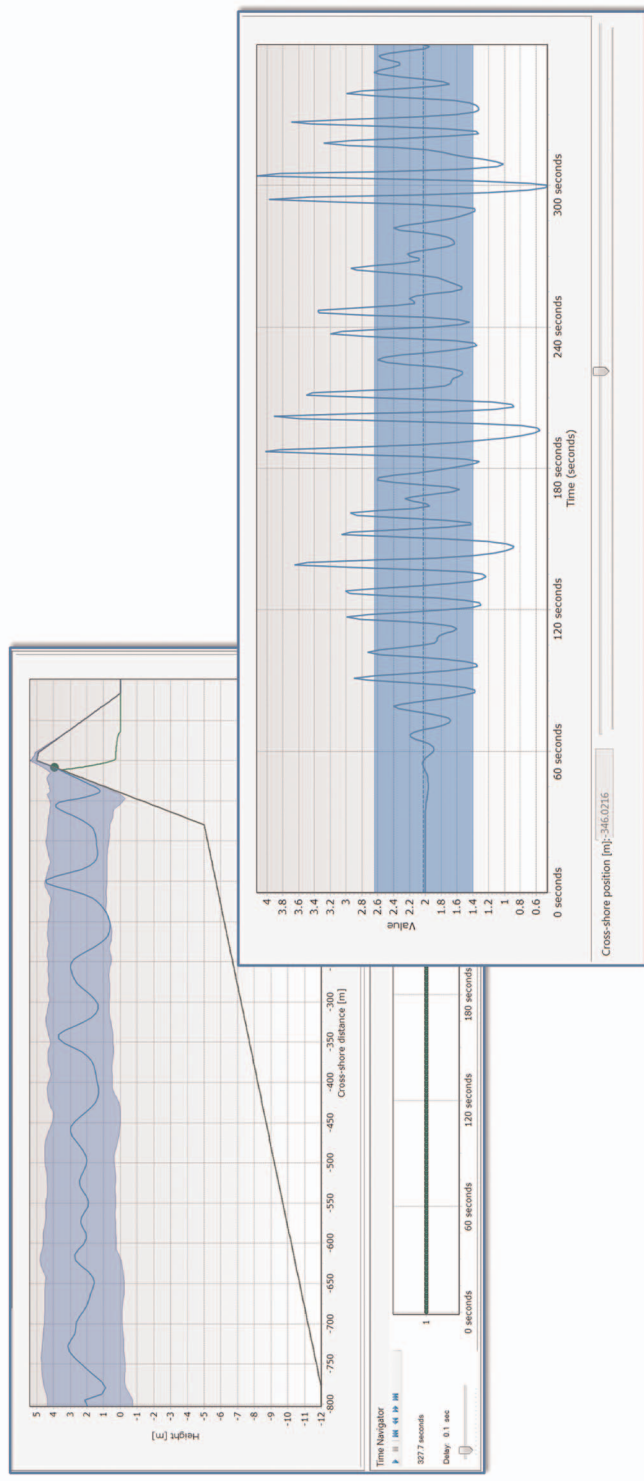
Maritime Engineering
Volume 167 Issue MA4

**Modelling storm response
on gravel beaches using
XBeach-G**
Masselink, McCall, Poate and
van Geer

Figure 6. An example of two output screens the GUI offers to analyse the output of XBeach-G model runs. The left view represents the cross-shore view, showing a cross-shore section of the output (gravel barrier in dark green; water surface elevation in blue; beach groundwater table across the barrier in light green; and the instantaneous shoreline or run-up indicated by the green circle) at $t = 304 \cdot 5$ s, which can be adjusted to using the time navigator controls at the bottom. The right view represents the time series view, showing an example of the water surface elevation time series at a specific location ($x = -554 \cdot 5$ m), which can be adjusted using the cross-shore position controls at the bottom

Maritime Engineering
Volume 167 Issue MA4

Modelling storm response
on gravel beaches using
XBeach-G
Masselink, McCall, Poate and
van Geer

calculation engine will then be written to the specified output location. This enables the user to run XBeach-G calculations elsewhere, for example on a calculation cluster, or write a script that uses the input file to run calculations in batch mode, changing one or more of the input parameters. When finished running these calculations, it is also possible to import the calculation results back into the GUI environment. XBeach-G calculation output can be stored in a single file. When using the import functionality for the results, this output file is coupled to a model set-up already specified in the GUI environment (and, for example, also used to export the model set-up). Calculation results can then be analysed as if the calculations were run inside the environment of the GUI.

5.   Model application

5.1   Reshaping the Slapton Sands barrier to prevent overwash

The 5 km-long gravel barrier system of Slapton Sands is located on the south Devon coast (Figure 7(a)). A road runs along the crest of the barrier, and the barrier is backed by a freshwater lagoon. The barrier was overtopped in 2001 and 2004, and overwashed in 2013, and there is mounting concern over the long-term integrity of the barrier system, and therefore the viability of the road and the freshwater status of the lagoon. In this case study XBeach-G will be used to look at the response of the barrier systems to extreme wave and water-level conditions, and explore the efficacy of two types of gravel nourishments as a means of preventing overwash.

For the model simulations the actual profile of Slapton Sands, representative of the central section of the barrier system, was uploaded with the seaward profile extrapolated to a depth of -12 m ordnance datum Newlyn (ODN; which is $\sim0{\cdot}2$ m below MSL) with a seaward slope of 1/10. The elevation of the barrier crest is ~6 m ODN and the supratidal part of the barrier is ~50 m wide. The existing barrier profile was modified by adding 25 m^3 per unit metre beach width to the profile (Figure 7(b)). In the first case, the sediment was added to the front of the barrier in the form of a wedge, extending the 6 m ODN contour 10 m seaward and increasing the gradient of the upper barrier to 1/8. In the second case, a 0·5 m cap was placed over the 50 m wide barrier crest region.

All three barrier profiles were subjected to the same extreme wave and water-level conditions, and with the same model parameters. The sea level was 3·5 m ODN (spring high tide plus a 1:50 year storm surge), the lagoon water level was 3 m ODN (actual mean lagoon level), aquifer depth was -5 m ODN (approximate elevation of underlying peat layer), and the wave conditions were characterised by a significant wave height H_s of 5 m and a peak wave period T_p of 12 s. The other input parameters used were: sediment size $D_{50} = 0{\cdot}01$ m;

(a)
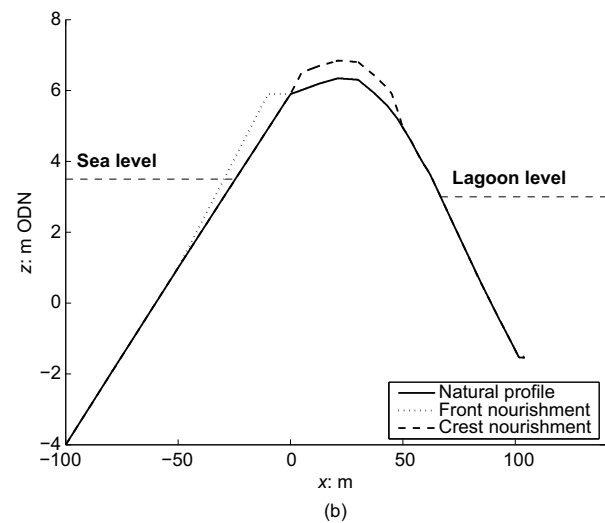
(b)

Figure 7. (a) Aerial photograph of the 5 km-long gravel barrier of Slapton Sands on the south coast of Devon, UK. (b) Natural profile of Slapton Sands and the modified profile due to nourishment placed on the front and the top of the barrier. Both nourishments represent 25 m^3 per unit metre beach width

hydraulic conductivity $K_{lam} = 0{\cdot}01$ m/s; and the default values for the sediment transport parameters. The run length for each test was 3600 s (1 h), to represent a sufficient period of time around a high tide to ensure significant morphological change occurs and robust extreme run-up estimates are obtained, and each of the three XBeach-G models was run with and without morphodynamic updating; the latter simulations were carried out to facilitate determining the effect of the morphology on the hydrodynamics without the confounding effects of changing morphology. It is noted that the morphodynamic modelling was conducted without prior calibration of the relevant sediment transport parameters; therefore, the results should be considered qualitative, not quantitative. In contrast

Maritime Engineering
Volume 167 Issue MA4

Modelling storm response
on gravel beaches using
XBeach-G
Masselink, McCall, Poate and
van Geer

to the simulations comparing observed with modelled run-up, which were repeated ten times with different random seeds of the wave spectra, the barrier response simulations were only conducted once for each case.

Figures 8(a)–8(c) shows the 1 h time series of modelled barrier overwash at the barrier crest location ($x = 20$ m). These runs were conducted without morphodynamic adjustment purely to look at the effect of different morphology on hydrodynamics. Perhaps surprisingly, the model run with the nourishment placed to the front of the barrier actually enhanced overwash intensity: more frequent overwashes and larger mean overwash volume (24 l/s/m compared with 17 l/s/m for the natural profile). Placing the nourishment on the crest of the barrier reduced the overwash frequency and the mean overwash volume (4 l/s/m). The model

runs with morphodynamic updating (Figures 8(d)–8(f)) all show retreat of the front of the barrier, significant deposition across the lower part of the profile and on the barrier crest, and a very small amount of back-barrier deposition ($\sim 0{\cdot}02$ m). Upper beach erosion and deposition across the lower part of the profile is largest for the profile with the nourishment to the front of the barrier. The barrier retreat for the upper beach of the profile ($z = 3$–6 m ODN) is ~ 7 m for the natural profile and the profile with crest nourishment, and ~ 12 m for the profile with the front nourishment, leaving the upper part of the latter profile ~ 5 m seaward of the other two profiles.

The reason for the enhanced overwash intensity and morphological change for the barrier profile with the front nourishment is that the steepening of the profile caused by the
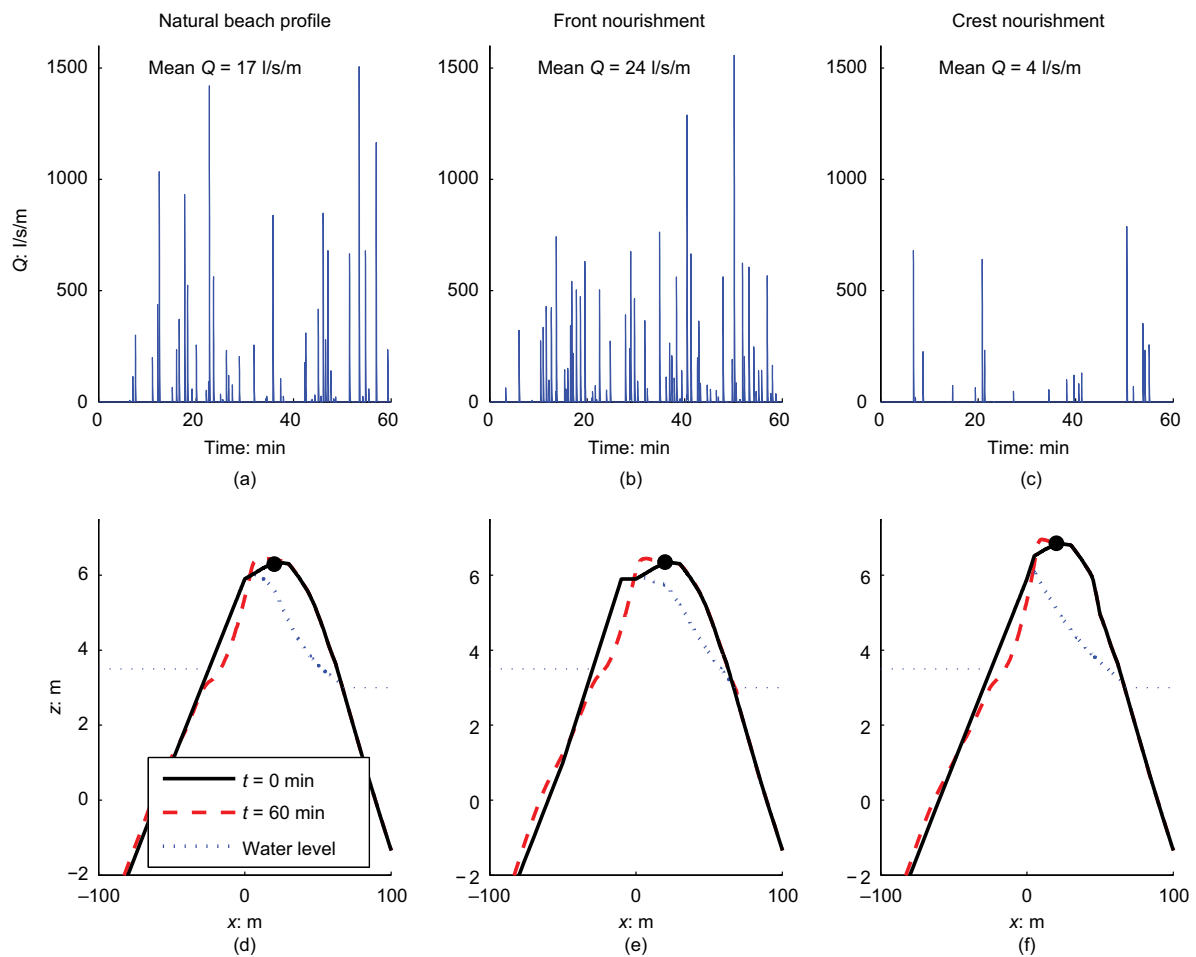

Figure 8. Modelled overwash and morphological response of the Slapton Sands gravel barrier when subjected to extreme wave and water-level conditions. (a–c) Overwash discharge time series for 1 h at the barrier crest ($x = 20$ m; indicated by the solid circle in (d–f)) for the three barrier profiles for runs without morphodynamic updating; (d–f) morphological response. (a, d) Natural Slapton Sands barrier profile; (b, e) natural profile with nourishment added to the front of the barrier; and (c, f) natural profile with nourishment added to the top of the barrier

Maritime Engineering
Volume 167 Issue MA4

**Modelling storm response
on gravel beaches using
XBeach-G**
Masselink, McCall, Poate and
van Geer

nourishment (from 1/10 to 1/8) leads to an increase in the vertical run-up. This is a very important factor that should be taken into account when using nourishment (or reshaping) as a coastal protection measure. The modelling further suggests that fixing the crest position of a retreating gravel barrier (e.g. due to sea-level rise) is unsustainable in the long run, because a steeper barrier becomes increasingly vulnerable to overwash.

5.2 Role of the shape of the wave spectrum

Along the south coast of England, it has been observed that coastal flooding caused by overwash is more likely to occur when energetic wind wave conditions coincide with a significant amount of swell wave energy; in other words, when the wave spectrum is bimodal (Bradbury, personal communication). The importance of swell energy and bimodality of the wave spectrum has also been highlighted by the work of Polidoro *et al.* (2013). The addition of a swell peak to a wind wave spectrum will automatically represent an increase in the wave energy and wave period, and therefore run-up, and it is therefore unclear whether the observed increase in the likelihood of overwash under bimodal wave conditions is simply due to an increase in wave energy and wave period, or is related to the bimodal nature of the wave spectrum. XBeach-G offers the opportunity to investigate whether run-up and overwash characteristics are significantly affected by the shape of the wave spectrum by allowing model simulations with differently shaped spectra (unimodal and bimodal), but identical significant wave height and mean wave period (H_s and T_m).

A total of eight XBeach-G models were set up using the 'idealised' barrier profile (cf. Figures 5 and 6), but with the water depth at the start of the profile extended from 15 to 20 m and the barrier height increased from 5 to 6 m), the input parameters listed in Table 1, a sediment size D_{50} of 0·01 m, a hydraulic

conductivity K of 0·01 m/s and the default values for the sediment transport parameters. The run length for each test was 3600 s (1 h). The four different test wave conditions represent widely varying spectral shapes (Figure 9(a)), but identical significant wave height H_s and mean wave period T_m (Table 1; T_m was computed as m_1/m_0, where m_1 and m_0 represent the first and zero moment of the wave spectrum, respectively). The peak periods T_p are also different, but it should be pointed out that for the bimodal wave condition of test T3 there is not a single spectral peak (moreover, spectral peak period strongly depends on the degree of smoothing of the wave spectrum).

During test series A (T1A–T4A), the water level was such that the swash motion was limited to the seaward slope of the barrier (MSL at 0 m; no overwash) and the morphology was not updated. These tests were purely designed to investigate the effect of wave spectral shape on wave run-up. The results shown in Figure 9(b) reveal that as the swell-wave contribution increases from 0% to 50%, while keeping the overall wave energy level and the mean wave period the same, the maximum wave run-up R increases from 3·35 to 5·12 m (50% increase). The maximum wave run-up is here defined as the average of the ten highest run-up events that occurred during the 1 h model simulation. This estimate of the extreme run-up level was found to be similar to, but more 'stable' than, the 2% exceedence level.

During test series B (T1B–T4B), the water level was raised to MSL at 3·5 m to ensure overwash occurred and morphodynamic updating was turned on. These tests were designed to investigate the effect of the wave spectral shape on overwash characteristics and morphological change due to overwash. The morphology before and after the model simulations for the four test wave conditions is presented in Figure 10. During all model simulations, erosion of the upper seaward slope of the barrier

Test	H_{s1}: m	T_{p1}: s	H_{s2}: m	T_{p2}: s	H_s: m	T_p: s	T_m: s	MSL: m	Morphological updating
T1A	5·0	10·0			5·0	10·0	8·6	0	No
T1B	5·0	10·0			5·0	10·0	8·6	3·5	Yes
T2A	4·5	9·3	2·2	15·0	5·0	9·3	8·6	0	No
T2B	4·5	9·3	2·2	15·0	5·0	9·3	8·6	3·5	Yes
T3A	4·0	8·4	3·0	15·5	5·0	8·5/15·5	8·6	0	No
T3B	4·0	8·4	3·0	15·5	5·0	8·5/15·5	8·6	3·5	Yes
T4A	3·55	7·3	3·55	16·0	5·0	16·0	8·6	0	No
T4B	3·55	7·3	3·55	16·0	5·0	16·0	8·6	3·5	Yes

MSL, mean sea level

Table 1. XBeach-G model parameters for investigating the influence of the shape of the wave spectrum on wave run-up and overwash characteristics

Maritime Engineering
Volume 167 Issue MA4

Modelling storm response
on gravel beaches using
XBeach-G
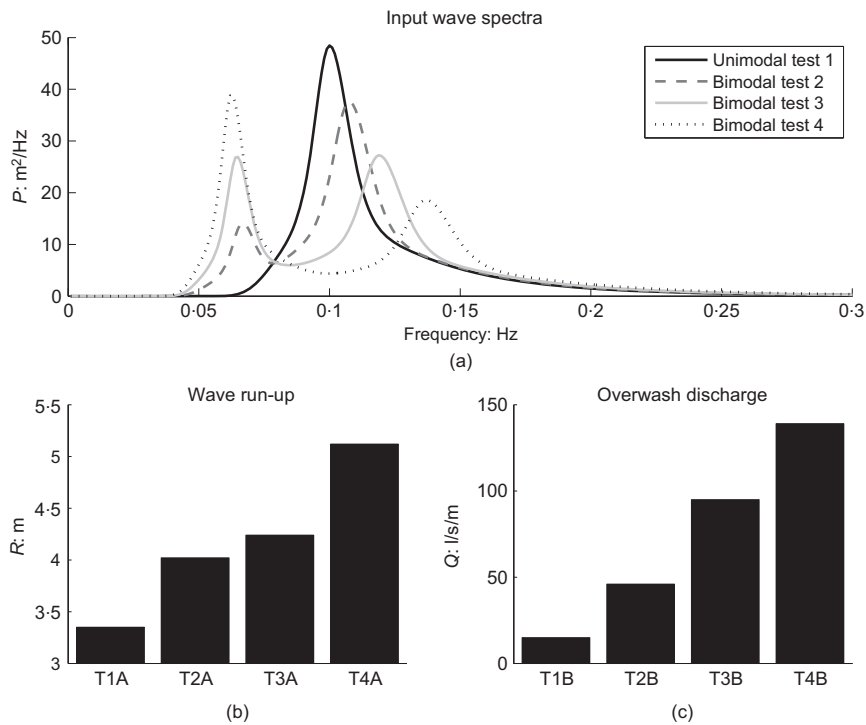Masselink, McCall, Poate and
van Geer

Figure 9. (a) Input wave spectra for investigating the role of spectral shape on wave run-up and overwash characteristics (for wave parameters refer to Table 1). (b) From left to right, maximum wave run-up R for test series A (T1A–T4A; no morphodynamic updating) and (c) mean overwash discharge Q across the crest of the barrier at $x = 0$ m for test series B (T1B–T4B; with morphodynamic updating)

occurs accompanied by deposition across the lower seaward slope (offshore sediment transport). The morphological response of the crestal region of the barrier differs, however, significantly between the different runs. During the test with unimodal wave conditions (T1B), some overwashing occurs, resulting in sediment deposition on the top of the barrier and a modest increase in the barrier crest height. However, for the tests with bimodal wave conditions (T2B–T4B) the increased intensity of the overwash process leads to enhanced shoreline retreat, barrier crest lowering and back-barrier deposition. The overwash intensity was quantified by determining the mean overwash volume across the barrier crest (at $x = 0$ m) and shows an almost tenfold increase from 15 l/s/m during T1B to 139 l/s/m during T4B (Figure 9(c)).

These model simulations highlight significantly different run-up and overwash characteristics for different wave spectral shapes, but identical H_s and T_m. Wave run-up and barrier overwash increases dramatically as the contribution of swell waves to the overall wave energy spectrum is increased. The increased run-up and overwash cannot be quantified by the peak wave period T_p (which decreases from T1 to T2 and is ambiguous for T3). The implication is that care should be taken in using run-up predictors based on simple wave parameters (e.g. Stockdon *et al.*, 2006).

6. Model capabilities and limitations
XBeach-G has been extensively validated for the prediction of storm-induced hydrodynamics (wave transformation, run-up, overtopping, overwash) on pure gravel beaches, and is able to simulate an observed morphological change on gravel beaches given correct model calibration. However, as XBeach-G is still under development, the model has important limitations that must be considered when applied to research, vulnerability and design projects. These limitations are discussed briefly below.

■ Morphodynamic calibration: although XBeach-G has been shown to be capable of reproducing observed morphodynamic change at the validation sites discussed in this paper and in McCall *et al.* (in preparation), calibration of the dominant sediment transport parameters will be required before application at other sites.
■ Longshore processes: XBeach-G has at this stage only been developed and validated as a one-dimensional cross-shore transect model. Although this is more computationally efficient than simulating processes in two-dimensional
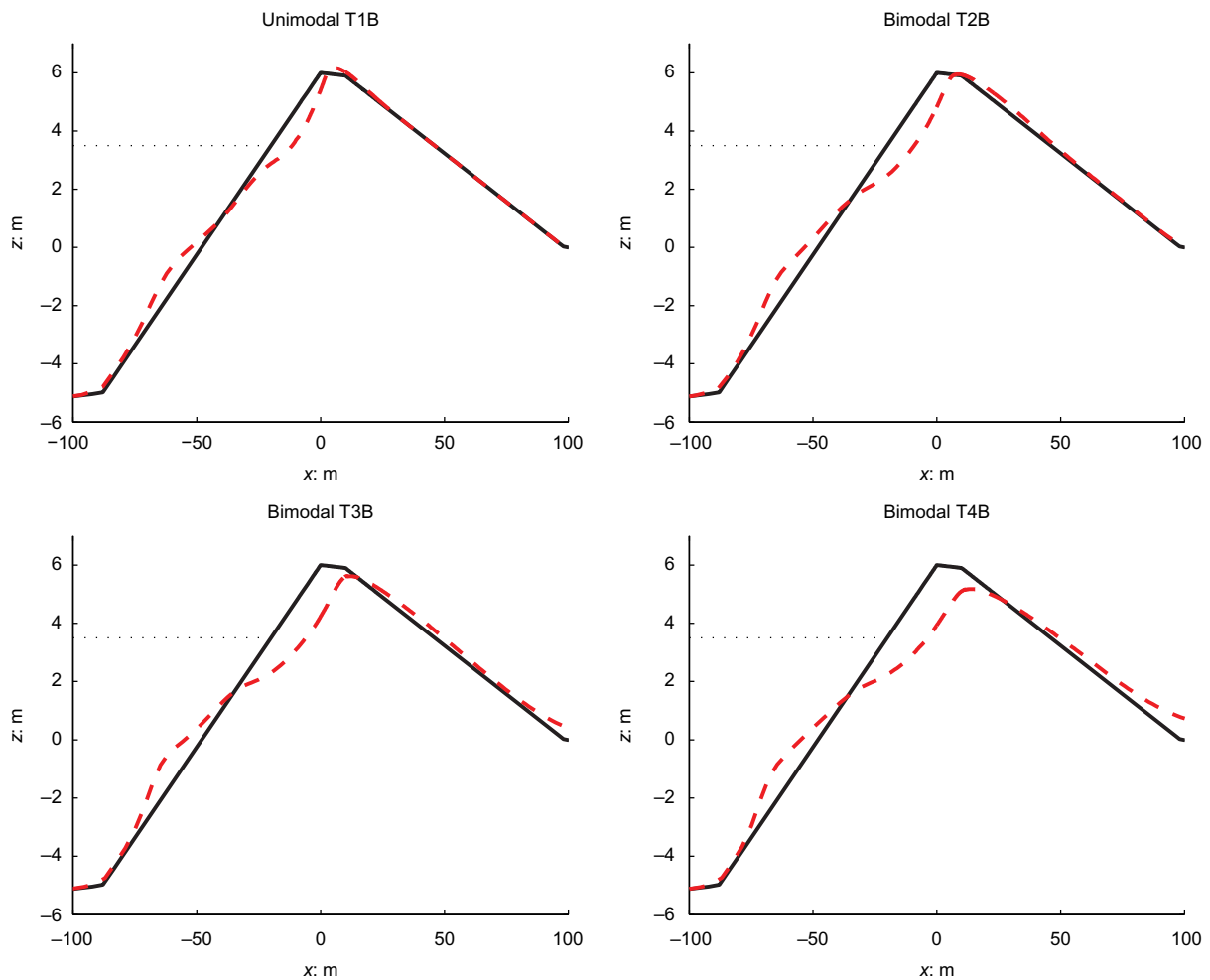
Maritime Engineering
Volume 167 Issue MA4

**Modelling storm response
on gravel beaches using
XBeach-G**
Masselink, McCall, Poate and
van Geer

Figure 10. Morphological response during 1 h of overwash
conditions for the wave conditions listed in Table 1. The black line
represents the morphology at the start of the simulation and the
red dashed line is the morphology at the end. The horizontal
dotted line is the mean sea level during the simulation

(2dH) (area model), an important limitation of this
schematisation is that the model assumes longshore
uniformity in forcing conditions and beach geometry. This
implies that XBeach-G will not compute longshore trans-
ports and, importantly, will not take into account sediment
gains and losses due to longshore transport gradients. It is
not recommended to apply the XBeach-G model in wave
conditions with a large angle of incidence ($>30°$ from shore
normal).

■ Wave transformation: the wave module of the XBeach-G
model has been shown to model wave transformation correctly
in the nearshore zone for shallow to intermediate water depths.
However, due to limitations in the processes modelled by the
wave module (e.g. wind-driven wave growth) and numerical
limitations of the wave module (e.g. numerical approximation

of the vertical pressure distribution, numerical diffusion) the
model cannot be used to model wave transformation
accurately from deep water or from large distances from the
shore. It is therefore recommended to apply XBeach-G in
shallow relative water depths ($kd < 3$, where k is the wave
number and d is the water depth) and over limited cross-shore
distances ($L_{model} < 20 L_{wave}$, where L_{model} is the cross-shore
model domain extent and L_{wave} is the characteristic wave
length).

■ Mixed sand–gravel beaches: XBeach-G has been designed
for use on pure gravel beaches and has not been tested on
mixed and composite sand–gravel beaches. Although
XBeach-G should be able to compute wave transformation
and wave run-up correctly on sand–gravel beaches given
correct schematisations for groundwater processes, the

Maritime Engineering
Volume 167 Issue MA4

Modelling storm response
on gravel beaches using
XBeach-G
Masselink, McCall, Poate and
van Geer

model does not contain sediment transport processes for (sandy) suspended sediment transport. The model is therefore currently not suitable for computing morphodynamic change on mixed sand–gravel beaches.

7. Conclusion

This paper presents an overview of one of the key results of the NUPSIG research project, which was aimed at developing the capability to predict the response of gravel beaches and barriers to extreme wave and water-level conditions. The XBeach-G model and the accompanying GUI will allow end-users to investigate the safety of gravel beaches and barriers against storm erosion and flooding, and assist in the development of coastline management and flooding mitigation plans. Example case studies discussed in this paper show the use of the XBeach-G model in accessing beach recharge schemes in terms of their effect on beach morphology during extreme conditions, and the use of the model in identifying the effect of the wave spectrum on storm wave overtopping thresholds. The XBeach-G model and GUI, as well as the XBeach-G model source code (Fortran95), are available for download on the XBeach project website (www.xbeach.org).

REFERENCES

Ardhuin F and Accensi M (2011) *Etats de mer et agitation sur le fond dans la sous-région marine Manche, Mer du Nord DCSMM/EI/MMN*. Ministère de l'Ecologie du Développement Durable des Transports et du Logement, Paris, France, Ref. DCSSM/EI/EE/MMN/1.1.7/2011 (in French).

Austin MJ and Masselink G (2006) Swash and groundwater interaction on a steep gravel beach. *Continental Shelf Research* **26(20)**: 2503–2519.

Boersma SM and Hoenderkamp K (2003) *Tregor*. IFREMER, Amsterdam, the Netherlands.

Bradbury AP (2002) Predicting breaching of shingle barrier beaches – recent advances to aid beach management. *Proceedings of the 35th MAFF (DEFRA) Conference of River and Coastal Engineers*.

Bradbury AP, Cope SN and Prouty DB (2005) Predicting the response of shingle barrier beaches under extreme wave and water level conditions in Southern England. *Proceedings of Coastal Dynamics, ASCE, Barcelona, Spain*, pp. 1–14.

Buscombe D and Masselink G (2006) Concepts in gravel beach dynamics. *Earth Science Reviews* **79(1–2)**: 33–52.

Chadwick AJ, Karunarathna H, Gehrels WR et al. (2005) A new analysis of the Slapton barrier beach system. *Maritime Engineering* **158(4)**: 147–161.

Chanson H (2006) The Sillon de Talbert, Côtes d'Armor, North Brittany, France. *Shore and Beach* **74(3)**: 26–27.

Darcy H (1856) *Les fontaines publiques de la ville de Dijon*. Dalmont, Paris, France (in French).

Defra (Department for Environment, Food and Rural Affairs) (2011) *Science and Research Projects*. Defra, London, UK. See http://randd.defra.gov.uk/ (accessed 18/12/2014).

Donchyts G and Jagers B (2010) DeltaShell – an open modelling environment. *Proceedings of 2010 International Congress on Environmental Modelling and Software, Ottawa, Canada*.

Fredsøe J and Deigaard R (1992) *Mechanics of Coastal Sediment Transport*. World Scientific, Singapore.

Halford K (2000) Simulation and interpretation of borehole flowmeter results under laminar and turbulent flow conditions. *Proceedings of the 7th International Symposium on Logging for Minerals and Geotechnical Applications, Golden, Colorado, USA*. Minerals and Geotechnical Logging Society, Houston, TX, USA, pp. 157–168.

Heijne I and West G (1991) Chesil sea defence scheme. Paper 2: design of interceptor drain. *Proceedings of the Institution of Civil Engineers* **90(4)**: 799–817.

Jennings R and Shulmeister J (2002) A field based classification scheme for gravel beaches. *Marine Geology* **186(3–4)**: 211–228.

Kirk TM (1975) Mixed sand and gravel beaches: morphology, processes and sediments. *Progress in Physical Geography* **4(2)**: 189–201.

Komar PD (2010) Shoreline evolution and management of Hawke's Bay, New Zealand: tectonics, coastal processes, and human impacts. *Journal of Coastal Research* **26(1)**: 143–156.

López de San Román-Blanco B, Coates TT, Holmes P et al. (2006) Large scale experiments on gravel and mixed beaches: experimental procedure, data documentation and initial results. *Coastal Engineering* **53(4)**: 349–362.

Lorang MS (1991) An artificial perched-gravel beach as a shore protection structure. *Proceedings of Coastal Sediments*. American Society of Civil Engineers, New York, NY, USA, pp. 1916–1925.

Maritime Engineering
Volume 167 Issue MA4

Modelling storm response
on gravel beaches using
XBeach-G
Masselink, McCall, Poate and
van Geer

McCall RT, Masselink G, Roelvink J *et al.* (2012) Modeling
overwash and infiltration on gravel barriers. *Proceedings of
33rd International Conference on Coastal Engineering,
Santander, Spain.*

McCall RT, Masselink G, Poate TG *et al.* (2013) Predicting
overwash on gravel barriers. *Journal of Coastal Research*
65: 1473–1478.

McCall RT, Poate TG, Masselink G *et al.* (2014) Modelling storm
hydrodynamics on gravel beaches with XBeach-G. *Coastal
Engineering* **91**: 231–250.

Masselink G and Turner IL (2012) Large-scale laboratory
investigation into the effect of varying back-barrier lagoon
water levels on gravel beach morphology and swash zone
sediment transport. *Coastal Engineering* **63**: 23–38.

Meyer-Peter E and Müller R (1948) Formulas for bed-load
transport. *Proceedings of the 2nd Meeting of the International
Association for Hydraulic Structures Research*, pp. 39–64.

Moses CA and Williams RBG (2009) Artificial beach recharge: the
south east England experience. *Zeitschrift für
Geomorphology* **52(Suppl. 3)**: 107–124.

Nielsen P (2002) Shear stress and sediment transport
calculations for swash zone modelling. *Coastal Engineering*
45(1): 53–60.

Obhrai C, Powell KA and Bradbury A (2008) A laboratory study
of overtopping and breaching of shingle barrier beaches.
*Proceedings of the 31st International Conference on Coastal
Engineering*. American Society of Civil Engineers, New
York, NY, USA, pp. 1497–1508.

Poate TG, Masselink G, Davidson M *et al.* (2013) High frequency
in-situ field measurements of morphological response on a
fine gravel beach during energetic wave conditions. *Marine
Geology* **342**: 1–13.

Polidoro A, Dornbusch U and Pullen T (2013) Improved
maximum run-up formula for mixed beaches based on field
data. In *Coasts, Marine Structures and Breakwaters 2013:
From Sea to Shore – Meeting the Challenges of the Sea*
(Allsop W and Burgess K (eds)). ICE Publishing, London,
UK.

Powell KA (1990) *Predicting Short Term Profile Response for
Shingle Beaches*. HR Wallingford, Wallingford, UK,
Report SR 219.

Pye K and Blott SJ (2006) Coastal processes and morphological
change in the Dunwich – Sizewell area, Suffolk, UK.
Journal of Coastal Research **22(3)**: 453–473.

Pye K and Blott SJ (2009) Progressive breakdown of gravel-
dominated coastal barrier, Dunwich–Walberswick,
Suffolk, UK: processes and implications. *Journal of Coastal
Research* **25(3)**: 589–602.

Roelvink JA, Reniers A, van Dongeren AJHM *et al.* (2009)
Modelling storm impacts on beaches, dunes and barrier
islands. *Coastal Engineering* **56(11–12)**: 1133–1152.

She KM, Horn DP, Trim L and Canning P (2007) Effects of permeability
on the performance of mixed sand-gravel beaches. In

*Proceedings of the International Conference on Coastal
Sediments* (Kraus NC and Rosati JD (eds)). American Society
of Civil Engineers, New York, NY, USA, pp. 520–530.

Simm JD (1991) *Manual on the Use of Rock in Coastal and
Shoreline Engineering*. CIRIA, London, UK. CIRIA
special publication 83, CUR Report 154.

Smit P, Stelling G, Roelvink JA *et al.* (2010) *XBeach: Non-
hydrostatic Model: Validation, Verification and Model
Description*. Delft University of Technology, Delft, the
Netherlands.

Smit P, Zijlema M and Stelling G (2013) Depth-induced wave
breaking in a non-hydrostatic, near-shore wave model.
Coastal Engineering **76**: 1–16.

Stéphan P, Suanez S and Fichault B (2010) Franchissement et
migration des cordons de galets par rollover. Impact de la
tempête du 10 mars 2008 dans l'évolution récente du Sillon
de Talbert (Côtes-d'Armor, Bretagne). *Norois* **2015(2)**: 52–
58 (in French).

Stéphan P, Suanez S and Fichaut B (2012) Long-term
morphodynamic evolution of the Sillon de Talbert gravel
barrier (Brittany, France). *Shore and Beach* **80(1)**: 19–36.

Williams J, de Alegria-Arzaburu AR, McCall RT and van Dongeren
A (2012) Modelling gravel barrier profile response to
combined waves and tides using XBeach: laboratory and
field results. *Coastal Engineering* **63(May)**: 62–80.

Zijlema M, Stelling G and Smit P (2011) SWASH: an operational
public domain code for simulating wave fields and rapidly
varied flows in coastal waters. *Coastal Engineering* **58(10)**:
992–1012.